PROCESSING PARAMETERS FOR SELECTIVE LASER MELTING (SLM) OF GOLD

M. Khan and P. M. Dickens
Rapid Manufacturing Research Group, Loughborough University
Loughborough, United Kingdom

Abstract

Research into laser processing of different metals has enabled Solid Freeform Fabrication (SFF) processes to produce parts for a wide variety of applications. However, less focus has been made on the processing of precious metals. Currently little research has been reported on the processing of precious metals and alloys using the Selective Laser Melting (SLM) process. Here we present an initial investigation into the processing of 24 carat gold (Au) powder using a SLM system. Gold powder was tested for apparent density, tap density, particle shape and size distribution. A quality check of the specimen was carried out using a Scanning Electron Microscope (SEM) for sinterability and occurrence of porosity. Significant processing parameters were also identified.

1. INTRODUCTION

Laser based Solid Freeform Fabrication (SFF) processes like selective laser sintering (SLS), Laser Engineered Net Shaping (LENS^{TM}), Direct Light Fabrication (DLF), Direct Metal Laser Sintering (DMLS) and Selective Laser Melting (SLM) [1-6] induce flexibility into the production of intricate Three-Dimensional (3D) complex metallic parts. All of these processes vary either in the type of laser source (CO_2, lamp or diode Nd:YAG and fiber or disc lasers etc.) used or type of diffusion (sintering or melting) occurring in the thin layers of metallic powder. Research into the laser processing of different metals and alloys (e.g. aluminium, nickel, copper alloy, titanium and tool steel etc) has enabled these rapid manufacturing systems to produce parts for a wide variety of applications such as automotive, aerospace and medical implants etc. Gu and Shen [7] used copper powder to investigate balling phenomena in the DMLS process, Mumtaz et al [8] processed nickel based super alloy (Waspaloy®) using a high power pulse Nd:YAG laser system. Yadroitsev et. al. [9] processed Inconel 625 using Phenix System's PM 100 system. Simchi [10] sintered various ferrous powders: 316L stainless steel powder and M2 powders by EOS M250X^{tend} machine. Rombouts et al [5] investigated laser melting of different size and mixture of water and gas atomized steel powders. Simchi [11] also investigated particle size effect on the sintering of iron powders. Fischer et al [12] sintered commercially pure titanium powder using an Nd:YAG laser. However, less focus has been made on the processing of precious metals and alloys. Thorsson [13] sintered 18 carat gold powder using EOS M250X^{tend} machine to fabricate jewellery items. Currently very little research has been reported on the processing of precious metals and alloys using the SLM process. Precious metals and alloys such as gold, silver, platinum and their alloys could be used for different applications like jewellery and dental implants etc. These parts could be easily produced using the manufacturing flexibility provided by the SFF processes. This investigation gives an initial insight into the processing of gold powder using the SLM system.

2. MATERIAL CHARACTERISTICS

The material used was 24 carat gold (Au) powder.

2.1 Particle Size Distribution

Particle Size Distribution (PSD) of gold powder was carried out with the laser diffraction technique using a Malvern Mastersizer 2000. Gold powder was first dispersed in water but due to its poor dispersion, isopropanol was then used as the dispersing medium. The PSD results obtained using water as a dispersant showed the smallest particle size of around 5μm whereas smallest particle size obtained with isopropanol (Figure 1) was as low as 3.3μm. For confirmation of the results, PSD was performed again using isopropanol, which also gave the same results. This difference in the two particle sizes was attributed to the fact that gold powder does not disperse well in water as compared to isopropanol. This was evident from the visual observation of both these solutions, where the colour of isopropanol changed to mild yellow on addition of gold powder, where no such observation was made in water and gold powder was floating on top. The SEM images (Figure 2a-d) obtained for gold powder also suggests smallest particles size of around 3μm. Figure 2c (marked in circle) shows smaller satellite particles sticking to the larger particles forming agglomerates. When this agglomerated gold powder was added to water in the PSD analysis, it dispersed very little hence giving a maximum particle size of around 88μm. The same gold powder when added to isopropanol for PSD analysis was dispersed well and indicated a maximum particle size of around 46μm. The SEM images taken at different points in the gold sample did not show any particles of around 85μm but particles around 45μm were abundant.

d(0.1): 10.403 um   d(0.5): 24.551 um   d(0.9): 46.734 um
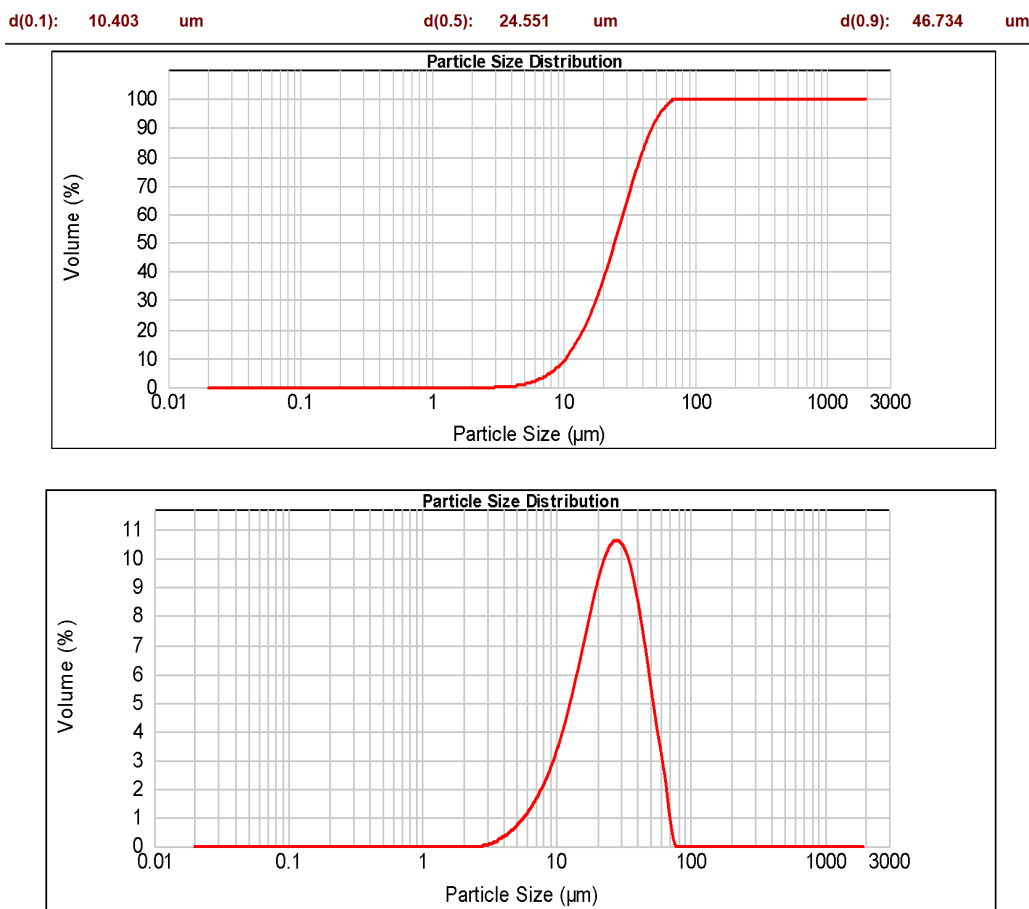

Figure 1: PSD of Gold (Au) Powder in Isopropanol

2.2. Scanning Electron Microscope (SEM) Analysis of Gold (Au) Powder

Figure 2 shows SEM images of gold powder. Gold (Au) powder was found to be mostly spherical in shape with smaller satellite particles agglomerated to the larger particles as shown in Figure 2c.
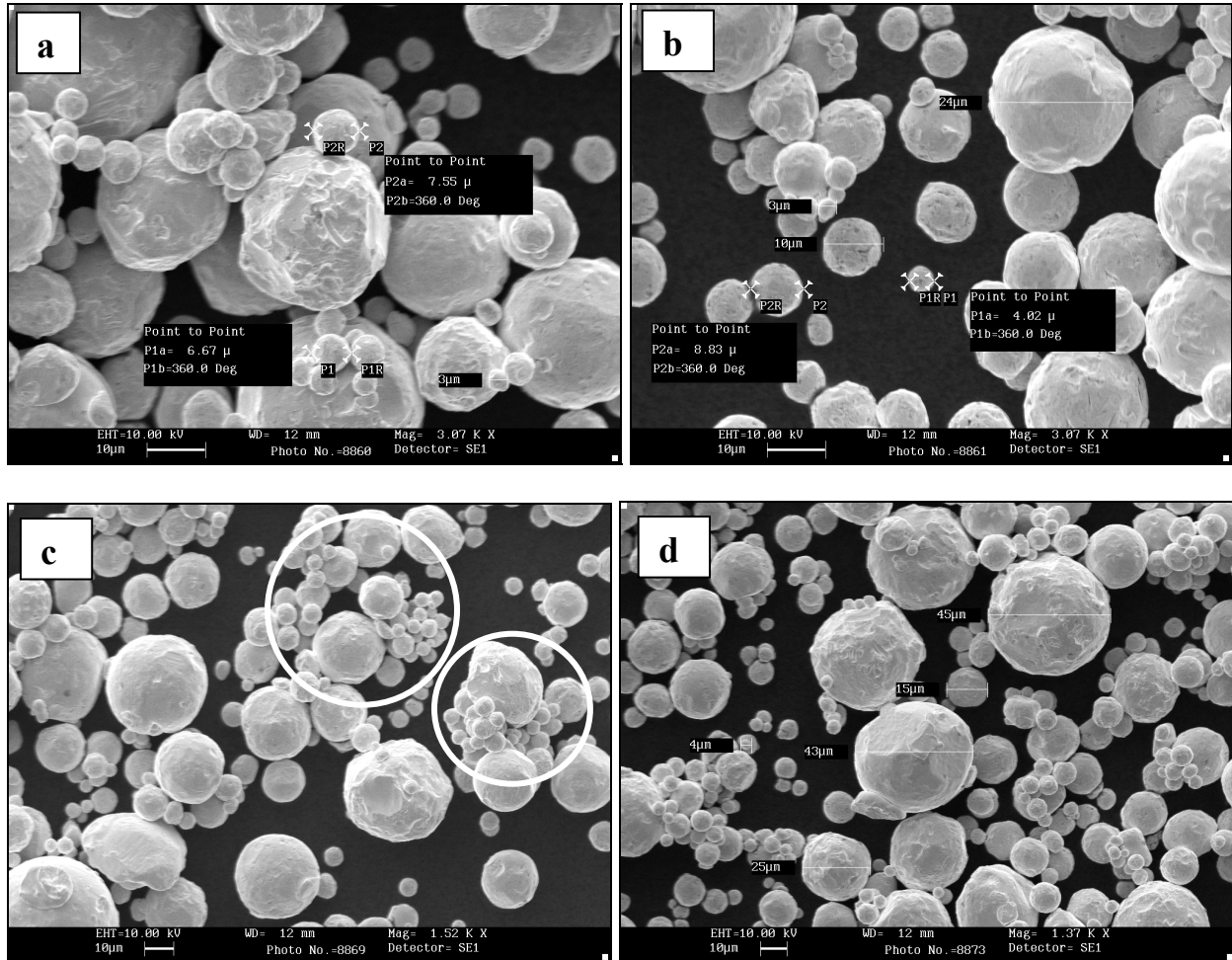

Figure 2 (a-d): SEM Images of Gold (Au) Powder

2.3 Apparent Density Measurements

The apparent density of powder is the density of powder in its loose state in a fixed size container [14]. Powder's apparent density or green density is of great importance in layer-based Rapid Manufacturing (RM) processes. Zhu et al [15] showed that apparent density or green density of the powder bed directly influences final density of the sintered parts. The higher the density of powder bed, then the higher will be the density of final sintered parts.

Here, gold powder was initially tested for apparent density according to ASTM B212-99 [16], ASTM B417-00 [17], BS EN 23923-1:1993 [18] and ISO 3923-1:1979 [19] standards. These standards use a Hall flowmeter funnel and Carney Funnel with an orifice of 2.5 and 5mm respectively (depending on the flowability of metal powder through 2.5 or 5 mm orifice). It was found that gold powder did not flow freely though the Hall flowmeter funnel. In the Carney funnel, even with the assistance of a metallic wire through the funnel, gold powder was very

reluctant to flow and would stop flowing as the metallic wire stopped moving. Therefore, ASTM B329 [20], BS EN 23923-2 [21] and ISO 3923-2 [22] standards were adopted which specify the apparent density measurement method for powder not flowing freely through a 2.5 or 5mm orifice funnels. The equipment used for measuring apparent density of gold powder was the Scott Volumeter [23] (as shown in Figure 3). Apparent density was measured with the standard 25cm^3 density cup and two other cups with different height-to-diameter aspect ratios. These cups were used to check the variation in apparent density with change in the dimensions of the density cups. It is known that the pouring height (shielded and non-shielded) of the powder also influences its apparent density measurements [24], therefore gold powder was poured from a fixed height (as specified in the standards) for all measurements.
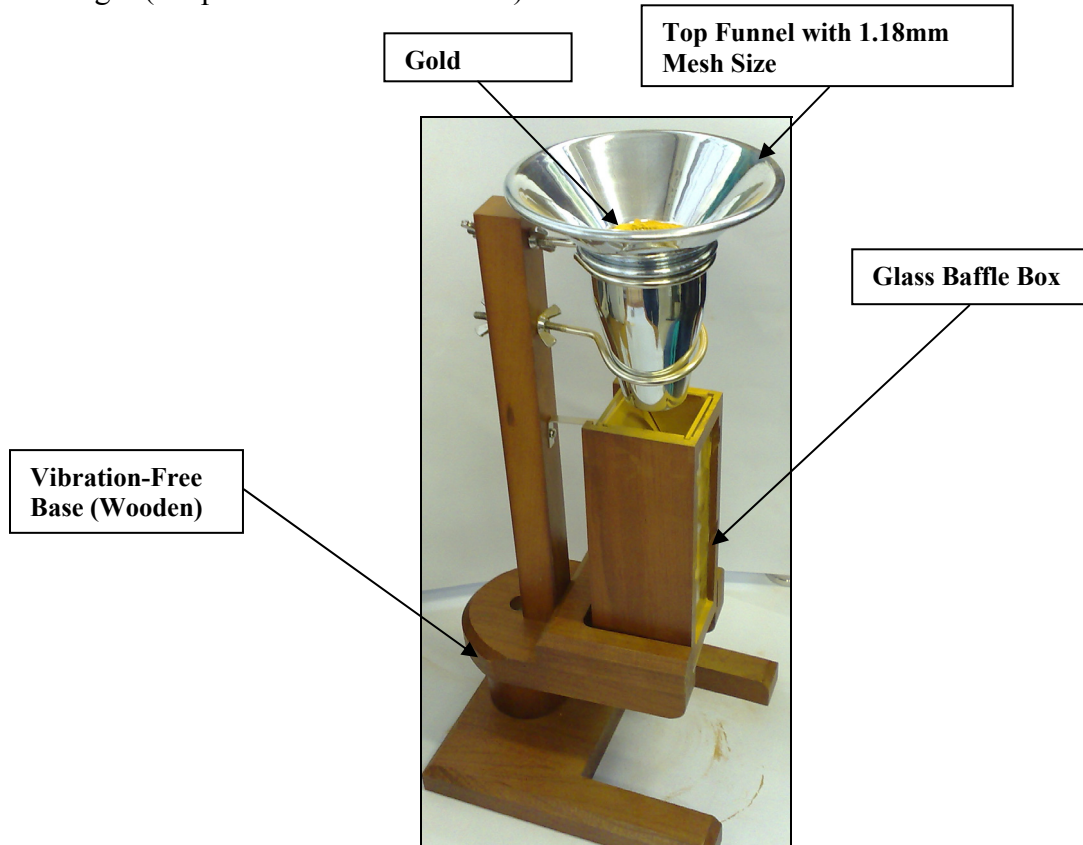

Figure 3: Scott Volumeter

The apparent density experiments were performed according to the standard and then a non-standard method. With the standard method, a 25 cm^3 brass density cup was first weighed on a digital balance (accuracy of $\pm$ 0.05 g). Gold powder was then added to the top hopper of the Scott volumeter and with the use of a nylon brush gold powder was assisted to flow through a 1.18mm mesh size sieve. A glass slab was used to scrape the extra powder from the top of the 25 cm^3 density cup as carefully as possible so as not to disturb the cup and weighed on a digital balance. The weight of the sample was calculated from the difference of the two readings (with and without metal powder).

With the non-standard method, apparent density experiments were also conducted with two stainless steel cups with different height-to-diameter aspect ratio. Table 1 specifies the

aspect ratio and volume of all the density cups used to measure apparent density of gold powder including the standard 25cm^3 brass density cup.

Table 1: Aspect Ratio of Density Cups

S/NO	Aspect Ratio	Description	Volume (cm^3)
Cup # 1	0.5	Stainless Steel Density Cup	10
Cup # 2	1.5	Standard Brass Density Cup	25
Cup # 3	2	Stainless Steel Density Cup	9

Figure 4 shows variation in the apparent density for different aspect ratio density cups. It was noted that these variations in the cup dimensions (height and diameter) had almost negligible effect on the apparent density of gold powder.
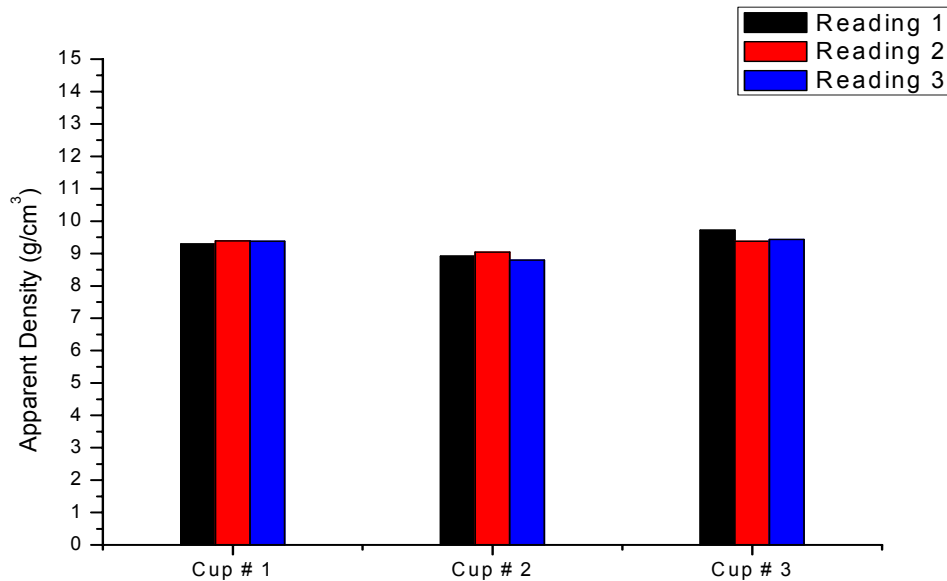

Figure 4: Apparent Density with Different Aspect Ratio Density Cups

2.4 Tap Density Measurements

The increase in the mean particle size has a great influence on the arrangement of particles as they try to form a dense packing [25]. During tapping or agitation of powder for compaction, smaller and larger particles re-arrange themselves to form a dense packing. Increasing the percentage of larger particles provide more inter-particle space for smaller particles to fill in. However, most of the smaller particles tend to go downward to the bottom of the density cup hence leaving more voids in the middle and upper section of the cup [26]. Tap density of the gold powder was determined by two different methods i.e. Constant Weight Tap Density (CWTD) method and Constant Volume Tap Density (CVTD) method.

2.4.1 Constant Weight Tap Density (CWTD) Method

The CWTD method is according to the ASTM B527 [27] and BS EN ISO 3953 [28] standards where tapping was performed by a manual method. As the apparent density of gold powder was greater than 7g/cm^3, so according to tap density standards for metallic powders, the

mass of the gold sample needed was 100g. A 100g sample of gold powder was weighed on a digital balance (accuracy ±0.05g) and poured gently into the standard 25 cm^3 graduated glass cylinder to avoid any compaction of powder before tapping. It was also ensured that powder formed a horizontal level in the cylinder so that it could be easily measured. A total of 200 taps were performed for each sample with the manual method (according to BS EN ISO 3953:1995) using a hard rubber pad. The volume of the samples was measured directly from the readings on the standard 25cm^3 graduated cylinder to give the tap density after a specific number of taps. If the powder was not level in the cylinder then the average of the maximum and minimum value was taken as the tap density reading. Each of the experiments was performed three times to check repeatability of the results.

Figure 5 shows an increase in the tap density of gold powder with increasing number of taps for a standard 25cm^3 graduated glass cylinder. It can be noted that after 60 taps gold powder was almost completely compacted thereby reaching its maximum tap density. There was found to be very little variation in the tap density after 60 taps. Figure 5 follows a typical tap density curve where powder is compacted quickly in the initial taps while less variation is observed after it reaches its maximum compaction.
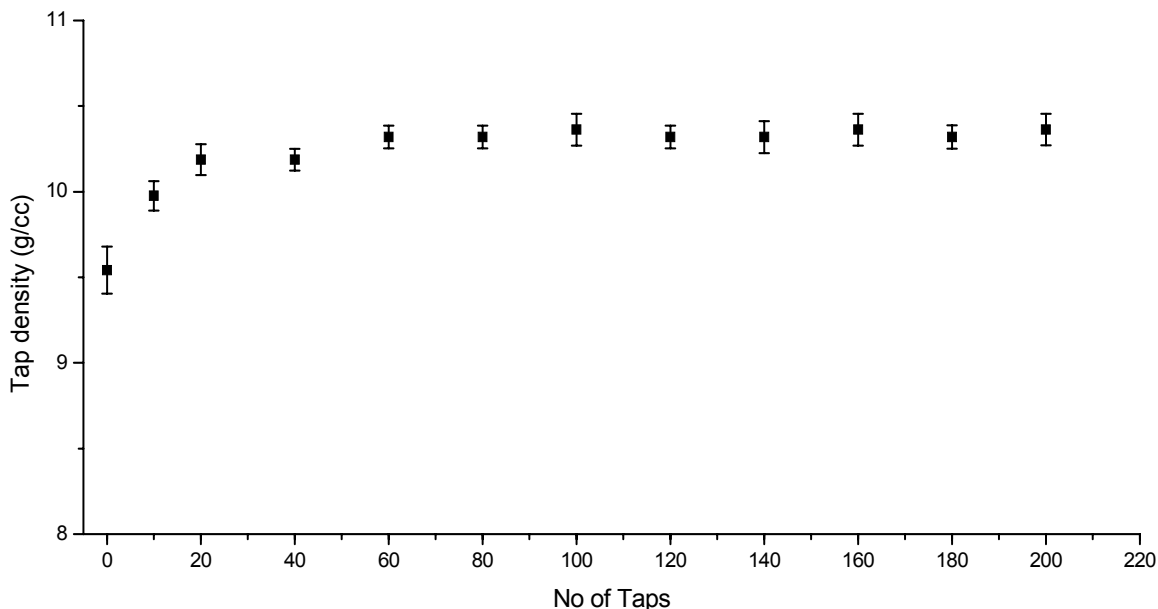

Figure 5: Tap Density of Gold Powder with CWTD Method

2.4.2 Constant Volume Tap Density (CVTD) Method

In contrast to the standard method of tap density measurement (CWTD method) in which mass of the test sample is fixed (100g in the case of gold powder), the CVTD method used a fixed volume of the test sample. In this method three density cups with different height-to-diameter aspect ratio (as shown in Table 1) were used to measure tap density, which were also used for apparent density measurements. All the density cups were weighed on a digital balance (accuracy of ± 0.05 g). Powder was poured through Scott volumeter into the density cups. Excess powder was scraped with a glass slab and weighed. Extension pieces were placed and powder was added again from the Scott volumeter. The density cups were tapped and after removing the extensions the excess powder was scraped and the cups were weighed to give the tap density

after specific number of taps. Figure 6 shows the CWTD of standard 25cm^3 graduated glass cylinder and CVTD of Cup # 1, Cup # 2 and Cup # 3. It is noted that there is very little difference between the tap densities measured by CWTD and CVTD methods. Both in CWTD and CVTD methods, there is a jump between the first and second reading which indicates that gold powder compacted very quickly initially while after 60 taps the density remained almost constant.
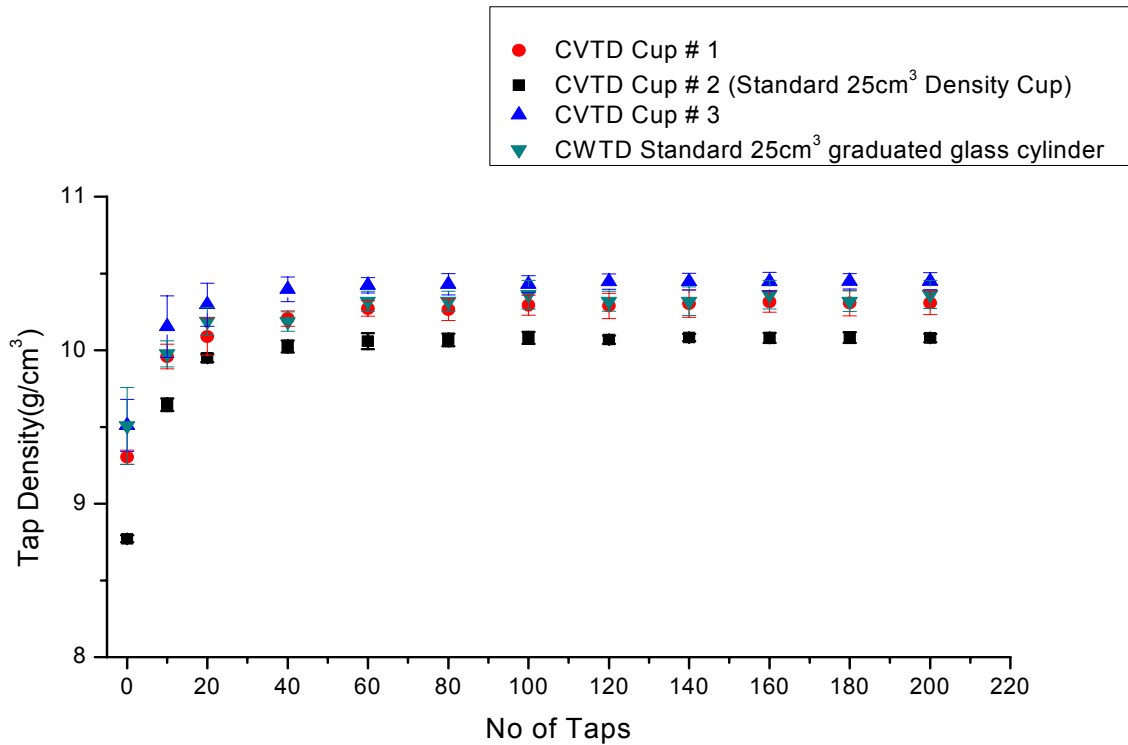

Figure 6: CVTD and CWTD for Different Density Cups

3. LASER SINTERING

3.1 Experimental setup

A SLM 100 system was used to process gold powder. The SLM 100 system uses a 50 watts continuous wave ytterbium fibre laser at a wavelength of 1070 to 1090nm. The SLM 100's scanning system incorporates an f-theta lens and uses the same layered based techniques as the majority of the other SFF processes. In the SLM 100 a wiper spreads single layer of powder on the surface of a 125mm diameter steel substrate followed by the fiber laser scanning a single cross-sectional layer of the part. This process is repeated multiple times to create 3-dimesional metallic parts. Having a very small laser spot size (as small as 25μm) and smaller build area, the SLM 100 is highly suitable for processing precious metals and alloys. The SLM 100 is also ideally suited for highly detailed and customized small parts such as jewellery items and dental crowns and implants etc. Figure 7 shows the SLM 100 setup.
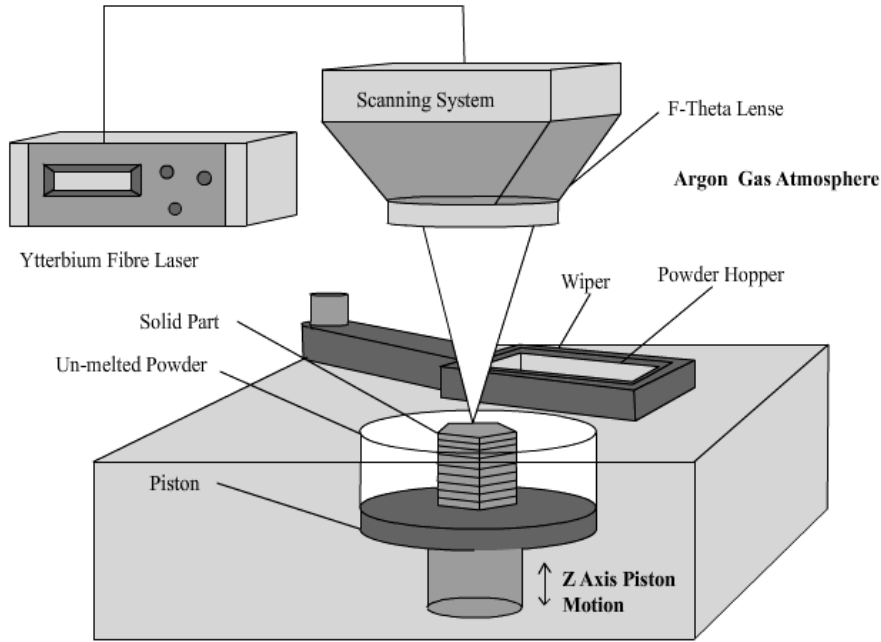
Figure 7: SLM 100 Setup

3.2 Scan Strategy

Processing of gold powder was carried out by two different scanning strategies. Figure 8a and b shows single-scan and cross-scan strategy for processing a single layer. In both the figures, a boundary scan (outer circle) was followed by a fill contour scan (inner concentric circle) while the solid area was scanned by hatch lines. In Figure 8a the whole area was scanned only once by single lines while in Figure 8b, the inner area was scanned two times by cross scanning.
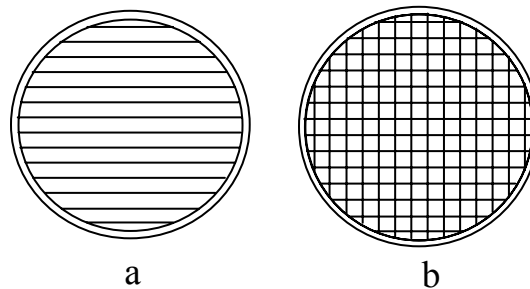

a   b

Figure 8: (a) Single-scan strategy and (b) Cross-scan strategy

3.3 Processing Parameters

A Laser power of 50 watts and hatch distance of 80µm was used in combination with different scanning speeds for boundary, fill contour and hatch solid to produce single layers. Processing parameters for gold (Au) powder are summarized in Table 2.

Table 2: Processing Parameters for Gold (Au) Samples

Processing Parameters		
Laser power		50 Watts
Scan speed	Boundary solid	250 mm/s
	Fill contour solid	250 mm/s
	Hatch solid	150 mm/s
Percentage overlap		72%
Hatch distance		80µm

4. RESULTS AND DISCUSSIONS

Different processing parameters such as laser power (watts), scan speed (mm/s), hatch distance (mm) and percentage overlap all hold an impact upon the formation of material processed using the SLM process. Figure 9 indicates the hatch scans, hatch distance, boundary scan and contour fill scan on the gold sample. Boundary scan represents the outer scan of each cross section of the part whereas contour fill scans represents all the inner scans parallel to the boundary scan. Boundary scan parameters influence the outer surface quality of the part in z direction.
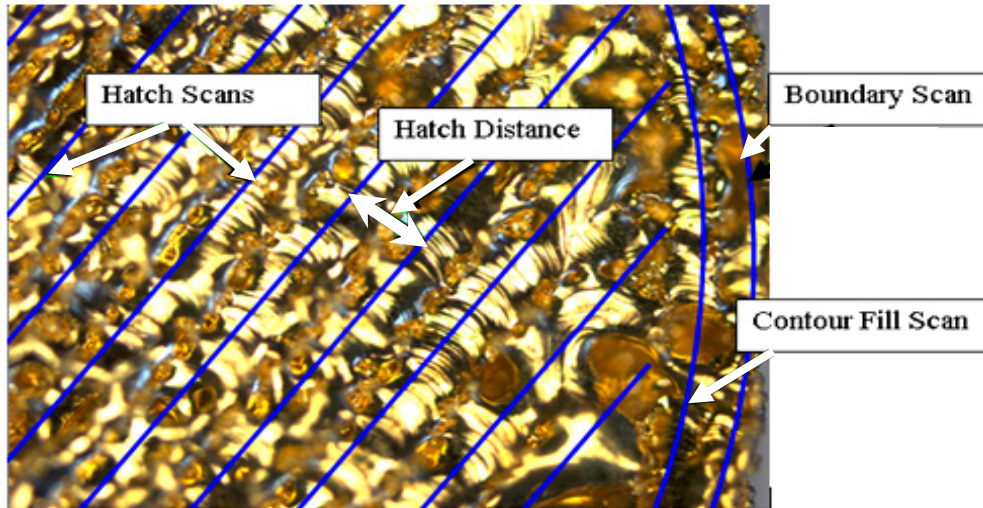

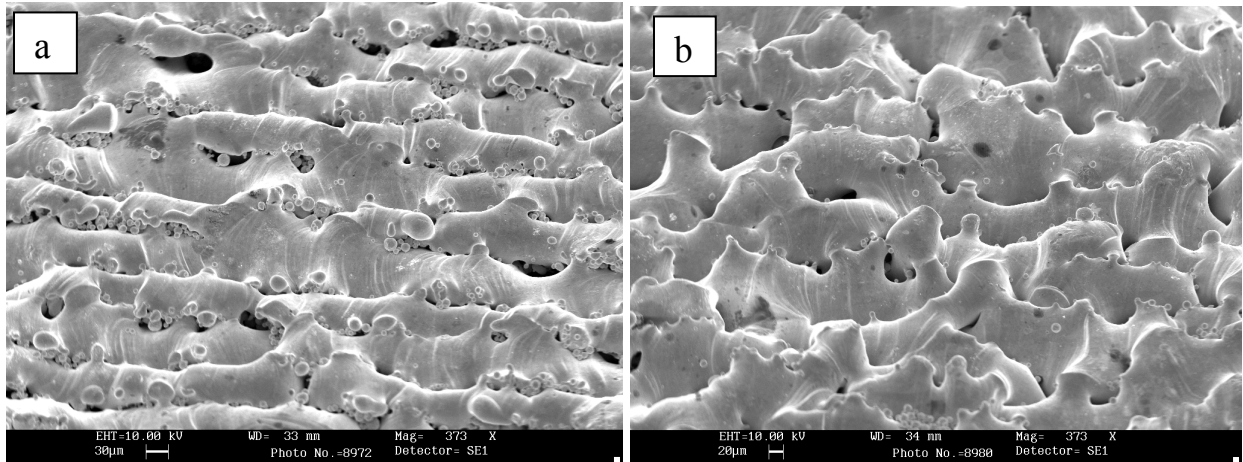Figure 9: Optical Microscope image of single scan gold (Au) layer

Figure 10: SEM images of scanned single layer of gold powder (a) single-scan strategy and (b) cross-scan strategy

Figure 10 (a and b) shows SEM images of a single layer of gold after a single-scan and cross-scan strategy using the SLM 100 system. Here, gold particles were completely melted to form a solid structure. The interconnected porosity is quite evident from these images. It can be seen that a single-scan surface shows a much more linear structure as compared to the cross-scanned sample surface. Some gold particles were sticking to the melted lines in the single-scan strategy whereas in cross-scan strategy almost all the particles were completely melted. The cross-scanned surface was more irregular (greater number of peaks and valleys) as compared to the single-scan surface.

4.1 Layer Thickness and Surface Morphology

The majority of the Rapid Manufacturing processes are layer based processes and therefore quality of a single layer such as layer thickness and layer surface profile plays a vital role in the quality of the final product. If the initial layer in producing a component is irregular and non-uniform then the following layers will be distorted, which could result in problems like porous structures and layer de-bonding etc. Here, layer thickness measurements of single-scan and cross-scan gold samples were conducted using a Talysurf CLI 2000 (Taylor Hobson Ltd) and was taken as the average of the three readings. Layer thickness of cross-scan layer (358µm) was found to be much greater than single-scan layer (278µm) due to the extra powder melting on second laser scanning in the cross-scan strategy. Also, as gold samples were produced on a thick powder layer and in the cross-scan strategy the same layer was scanned twice (with the same power and scan speed parameters) so more heat was dissipated into the powder thereby sintering more powder to the bottom side of the layer. Hence, this increased the layer thickness of the cross-scanned layer. Surface roughness measurements of the single-scan and cross-scan samples were performed using a Zygo and a Talysurf CLI 2000. A 300 x 300µm area was scanned at three different points on the samples (as shown in Figure 11). Table 3 shows the average surface roughness of single-scan and cross-scan layers. There is not much difference between the surface roughnesses of the two scan strategies. The surface morphology is quite different as could be seen in Figure 10 where the single-scan strategy (Figure 10a) produces more uniform surface with low peaks (Figure 10b. Figure 11a and b also shows surface profile of the gold samples.

Table 3: Surface Roughness and Layer Thickness of Single-Scan and Cross-Scan Gold (Au) Samples

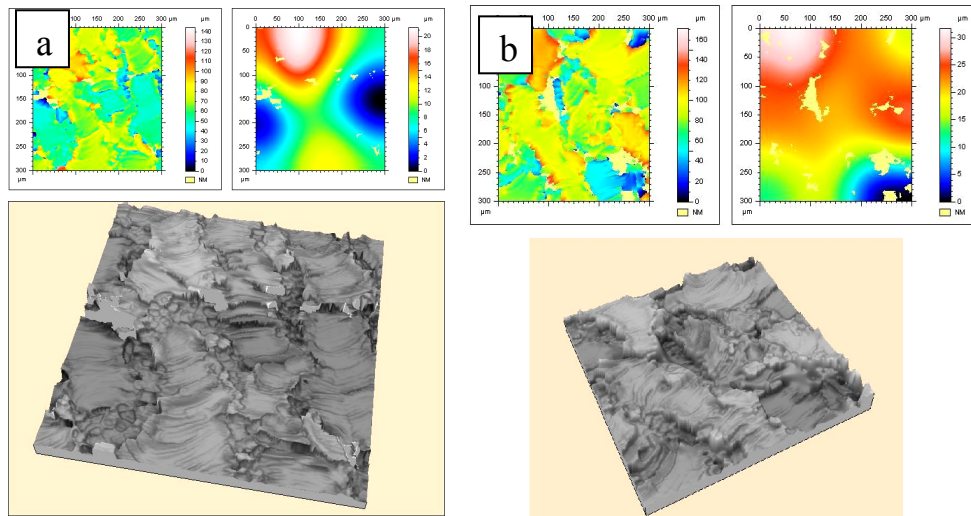| Scan Strategy	Average Surface Roughness (µm)	Average Layer Thickness (µm)
Single Scan	10.54	278
Cross Scan	13.08	358

Figure 11: 3D surface of (a) single-scanned and (b) cross-scanned gold (Au) layers

5. CONCLUSIONS

Initial investigation into the selective laser melting of gold powder was presented. Gold (Au) powder was tested for apparent density, tap density and particle size distribution.

1. Gold powder was found to be less dispersing in water as compared to isopropanol for PSD analysis, which was also confirmed by the SEM images and mean particle sizes.
2. Gold powder was found to be cohesive in nature and very difficult to flow through Hall and Carney funnels.
3. Smaller variation in the height-to-diameter aspect ratio of density cups had negligible effect on the apparent density and tap density of gold powder.
4. Layer thickness of a cross-scanned layer was found to be significantly greater than the single-scanned layer.
5. Surface morphology of the scanned gold layers was found to be effected by the two scanning strategies, whereas surface roughness was almost the same.

REFERENCES

[1] Liao, H. T. and Shie J. R. (2007), *Optimization on selective laser sintering of Metallic Powder via Design of Experiments Method,* Rapid Prototyping Journal, Vol. 13, Issue 3, pp 156-162, ISSN: 1355-2546

[2] Keicher, D.M., Miller, W.D., Smugeresky, J.E. and Romero, J.A., (1998), *Laser Engineered Net Shaping (LENS), Beyond Rapid Prototyping to Direct Fabrication,* Proceedings of the TMS Annual Meeting, San Antonio, TX, pp. 369–377

[3] Lewis, G.K., Nemec, R., Milewski, J., Thoma, D.J., Cremers, D. and Barbe, M. (1994), *Directed Light Fabrication,* Proceedings of the International Congress on Applications of Lasers and Electro-Optics, Orlando, Florida, USA, pp. 17–26

[4] Childs, T.H.C., Hauser, C. and Badrossamay, M. (2005), *Selective Laser Sintering (Melting) of Stainless and Tool Steel Powders*: *Experiments and Modelling,* Proceeding of IMechE, Part B: Journal of Engineering Manufacture, Vol. 219, Issue 4, pp. 339–357, ISSN: 0954-4054

[5] Rombouts, M., Kruth, J. P., Froyen, L. and Mercelis, P. (2006), *Fundamentals of Selective Laser Melting of alloyed steel powders,* CIRP Annals - Manufacturing Technology, Vol. 55, Issue 1, pp. 187–192, ISSN: 0007-8506

[6] Kruth, J. P., Mercelis, P., Vaerenbergh van, J., Froyen, L. and Rombouts, M. (2004), *Binding Mechanisms in Selective Laser Sintering and Selective Laser Melting,* Rapid Prototyping Journal, Vol. 11, Issue 1, pp. 26-36, ISSN 13552546

[7] Gu, D. and Shen, Y. (2007), *Balling Phenomena During Direct Laser Sintering of Multi-Component Cu-Based Metal Powder,* Journal of Alloys and Compounds, Vol. 432, Issue 1-2, pp.163-166, ISSN: 0925-8388

[8] Mumtaz, K. A., Erasenthiran, P. and Hopkinson, N. (2008), *High density selective laser melting of Waspaloy[®],* Journal of Materials Processing Technology, Vol. 195, Issue 1-3, pp 77-87, ISSN: 0924-0136

[9] Yadroitsev, I., Thivillon, L., Bertrand, Ph. and Smurov, I. (2007), *Strategy of manufacturing components with designed internal structure by selective laser melting of metallic powder,* Applied Surface Science, Vol. 254, Issue 4, pp 980-983, ISSN: 0169-4332

[10] Simchi, A. (2006), *Direct Laser Sintering of Metal Powders: Mechanism, Kinetics and Microstructural Features,* Materials Science and Engineering: A, Vol. 428, Issue 1-2, pp. 148-158, ISSN 0921-5093

[11] Simchi, A. (2004), *The Role of Particle Size on the Laser Sintering of Iron Powder,* Metallurgical and Materials Transactions B, Vol. 35, Issue 5, pp. 937-948, ISSN 1543-1940

[12] Fischer, P., Romano, V., Weber, H. P., Karapatis, N. P., Boillat, E. and Glardon, R. (2003), *Sintering of Commercially Pure Titanium Powder with a Nd:YAG Laser Source,* Acta Materialia, Vol. 51, Issue 6, pp. 1651-1662, ISSN 1359-6454

[13] Thorsson, L. (2006), *Laser Sintering of Gold Jewellery,* Proceeding of 1st International Conference on Rapid Manufacturing, 5-6 July, Loughborough, UK

[14] German, R. M. (1989), *Particle Packing Characteristics*, Metal Powder Industry, Princeton, New Jersey, ISBN: 0-918404-83-5

[15] Zhu, H. H., Fuh, J. Y. H. and Lu, L. (2007), *The Influence of Powder Apparent Density on the Density in Direct Laser-Sintered Metallic Parts,* International Journal of Machine Tools and Manufacture, Vol.47, Issue 2, pp 294-298, ISSN: 0890-6955

[16] American Society for Testing Materials (1999), *Standard Test Method for Apparent Density of Free Flowing Metal Powders using the Hall Flowmeter Funnel*, ASTM B212 (re-approved 2006)

[17] American Society for Testing Materials (2006), *Standard Test Method for Apparent Density of Non-Free-Flowing Metal Powders using the Carney Funnel*, ASTM B 417

[18] British Standard (1993), *Metallic Powders — Determination of Apparent Density— Part 1: Funnel Method*, BS EN 23923-1

[19] International Organization for Standardization (1979), *Metallic Powders — Determination of Apparent Density— Part 1: Funnel Method*, ISO 3923-1

[20] American Society for Testing Materials (1998), *Standard Test Method for Apparent Density of Free Flowing Metal Powders using the Scott Volumeter*, ASTM B329

[21] British Standard (1993), *Metallic Powders — Determination of Apparent Density— Part 2: Scott Volumeter Method*, BS EN 23923-2

[22] International Organization for Standardization (1981), *Metallic Powders — Determination of Apparent Density— Part 2: Scott Volumeter Method*, ISO 3923-2

[23] Scott, G. D. (1960), *Packing of equal spheres,* Nature, Vol. 188, pp. 908–909, ISSN: 0028-0836

[24] Santomaso, A., Lazzaro, P. and Canu, P. (2003), *Powder Flowability and Density Ratios: The Impact of Granules Packing*, Chemical Engineering Science, Vol. 58, Issue 13, pp. 2857-2874, ISSN: 0009-2509

[25] Svarovsky, L. (1987), *Powder Testing Guide: Methods of Measuring the Physical Properties of Bulk Powders*, Elsevier Applied Science Publishers Ltd., London and New York, ISBN: 1-85166-137-9

[26] Abdullah E. C. and Geldart, D. (1999), *The Use of Bulk Density Measurements as Flowability Indicators*, Powder Technology, Vol. 102, pp. 151-165, ISSN: 0032-5910

[27] American Society for Testing Materials (2006), *Standard Test Method for Determination of Tap Density of Metallic Powders and Compounds*, ASTM B527

[28] British Standard (1995), *Metallic Powders — Determination of Tap Density*, BS EN ISO 3953